Composites Part C: Open Access 14 (2024) 100453

Contents lists available at ScienceDirect

Composites Part C: Open Access

journal homepage: www.sciencedirect.com/journal/composites-part-c-open-access

Epoxy composite reinforced with jute/basalt hybrid – Characterisation and performance evaluation using machine learning techniques

Amith Gadagi [a], Baskaran Sivaprakash [b], Chandrashekar Adake [a], Umesh Deshannavar [c], Prasad G. Hegde [a], Santhosh P. [d,*], Natarajan Rajamohan [e], Ahmed I. Osman [f]

[a] Department of Mechanical Engineering, KLE Dr. M. S. Sheshgiri College of Engineering and Technology, Belagavi, Karnataka, India
[b] TamilNadu Government Polytechnic, Madurai, India
[c] Department of Chemical Engineering, Tatyasaheb Kore College of Engineering and Technology, Warananagar, India
[d] Department of Electrical and Electronic Engineering,University of Cagliari, Italy
[e] Chemical Engineering Section, Faculty of Engineering, Sohar University, Sohar, Oman
[f] School of Chemistry and Chemical Engineering, Queen's University Belfast, Belfast BT9 5AG, Northern Ireland, UK

ARTICLE INFO

Keywords:
Biofibre;POlymer;OPtimisation
Machine learning
Characterisation
Xgboost

ABSTRACT

Epoxy resins, prized for their versatile properties, are derived from bio-based materials, contributing to sustainability and eco-friendliness in both production and application. This study focuses on the application of gradient boosting machine learning techniques in the field of machining to predict the surface roughness and also the contour based experimental validation of the numerical results. The turning experiments, conducted via Taguchi's L_{27} array, aimed to explore the effects of depth of cut, feed rate, and spindle speed. Higher spindle speeds, lower feed rates, and shallower cuts led to smoother surfaces in turned jute/basalt epoxy composites. Machine learning models (Gradient Boosting Machine, AdaBoost, and XGBoost) were then used to predict surface roughness. Amongst these, XGBoost outperformed GBM and AdaBoost, exhibiting maximum and average prediction errors of 3.78 % and 2.24 %, respectively. XGBoost accurately predicted 2D surface roughness contours that closely matched experimental contours for training and test cases. Taguchi's Orthogonal Matrix identified minimum surface roughness values as 0.773 μm (experimental), 0.800 μm (GBM), 0.880 μm (AdaBoost), and 0.774 μm (XGBoost). All were achieved at 1500 rpm spindle speed, 0.05 mm/rev feed rate, and 0.3 mm depth of cut.

1. Introduction

Composites that integrate natural fibres with a polymer matrix or alternative binders define a distinct material category. Amongst these, jute fibres stand out for their affordability, abundance, and commendable mechanical properties. Widely employed across multiple industries-from textiles, construction, cosmetics, and medicine to packaging, automotive, and furniture-jute-based composites are derived from renewable sources, exhibiting biodegradability and a significantly reduced environmental impact. Their exceptional features, including sustainability, excellent insulation, and high tensile strength, have mainly propelled their extensive use in automotive and aerospace applications in recent times [1,2]. Epoxy resins, belonging to the prepolymer and polymer group, yield robust and versatile materials widely applied across various commercial and industrial sectors.

Jute-basalt epoxy hybrids are popular because of their exceptional strength, eco-friendliness, and biodegradability. Basalt, known for its high young's modulus and tensile strength, coupled with jute's excellent anti-static properties, enhances these composites resistance even at elevated temperatures, making them ideal for heat or fire exposure applications. Moreover, the synergistic combination of jute and basalt fibres imparts exceptional resistance to wear and abrasion, rendering these composites highly suitable for applications that prioritize durability. Researchers have extensively explored various aspects of jute-basalt epoxy hybrid composites, examining their mechanical properties, dynamic behaviours, and machining characteristics.Alshahrani et al. (2023) [3] designed a jute-basalt hybrid composite for automotive applications, exploring its young modulus, tensile strength, and bearing strength. Gangappa et al. (2023) [4] investigated jute-basalt epoxy composites' dynamic behaviour, compression strength, and tensile

* Corresponding authors.
E-mail address: santhosh.paramasivam@unica.it (S. P.).

https://doi.org/10.1016/j.jcomc.2024.100453

Available online 21 March 2024

modulus. Research study investigated incorporated graphene into basalt-jute epoxy composites, resulting in notable improvements in hardness, flexural, and tensile strength, with 55 %, 29 %, and 13 %, respectively [5].

The influence of drilling process variables in epoxy resin production is pivotal in determining crucial performance indicators like delamination factor, surface roughness, and thrust force [5–7]

Kishore, et al. [8] study on milling jute/basalt hybrid composites found significant process variable impacts on surface finish. Milling speed and feed notably affected delamination, roughness, and cutting force in jute-reinforced polymer composites. Notably, tool flute count also played a crucial role, with higher numbers correlating to reduced forces, roughness, and delamination [9].

Premkumar et al. [10].explored similar milling experiments on jute-reinforced polymer composites, finding that speed and feed influenced the delamination factor, surface roughness, and cutting force. Additionally, their investigation of the milling process characteristics of flax and jute fibre composites revealed that increasing spindle speed resulted in amplified delamination factor and vibration amplitude, whereas surface roughness and cutting force decreased. Performance indicators, including vibration amplitude, surface roughness, delamination factor, and cutting force, consistently increased with feed rate [11]. Rajendran et al. [12] leveraged grey relational analysis to optimize the depth of cut, speed, and feed rate for simultaneous minimization of tool wear, maximization of material removal, and target surface roughness in a single objective function.

Madara et al. [13].used the analysis of variance (ANOVA) approach to investigate the impacts of abrasive jet machining (AJM) process parameters on wear formation in Kevlar-jute epoxy hybrid composite specimens. Sridharan et al. [14].revealed superior drilling machinability in natural fibre composites compared to their synthetic counterparts and concluded natural fibre composites outperform synthetics in drilling machinability.Jain et al. [15].extended their exploration to laser beam machining of hybrid glass basalt composites, investigating delamination and pull-out phenomena resulting from the machining process.

Harun et al. (2016) explored milling parameter influence on fibre Reinforced Polymer surface finish via Taguchi optimization [16]. Their study identified feed rate and cutting speed as dominant factors dictating roughness, with lower feed rates and higher cutting speeds achieving superior surface finishes.Vinayagamoorthy et al. [17].developed a fuzzy logic model, a novel, predictive tool for drilling force prediction in natural hybrid composites.Meanwhile, Ramesh et al. [18]. drilling experiments on sisal-glass composites revealed how to drill types and feed rates significantly impact both thrust force and damage, highlighting the crucial role of parameter optimization..

Azuan et al. [19].evaluated the delamination tendencies of rice husk-reinforced polymer composites, noting that increased spindle speed and feed rates heightened delamination. Remarkably, delamination in rice husk-reinforced composites was lower thanin glass fibre composites. Sakthivel et al. [20]. developed a robust regression model that linked drilling variables in sisal-basalt composites with delamination and thrust force, paving the way for parameter optimization towards minimal thrust.

Jayabal et al. [21]. developed a regression model that predicts tool wear, thrust force, and torque in glass-coir-polyester drilling under varying process variables, particularly feed rate, which significantly impacts all three. The study further optimizes drilling parameters to enhance desired torque, thrust force, and tool wear performance in coir composites [22].

Debnath et al. [23] investigated the impact of spindle speed, feed rate, and drill geometry on damage and forces during sisal-fibre composite drilling. Meanwhile, AL-Oqla et al. [24] focused on sustainable biomass composites for the automotive industry, designing them using decision models that consider physical, mechanical, thermal, moisture resistance, and specific performance criteria.

Research into lignocellulosic materials has led to the fabrication of composites with similar characteristics. Investigations on their mechanical properties encompass fatigue, tensile, impact, and flexural strength, including studies on the influence of moisture and different environments [25,26]. Saba et al. [27].demonstrated enhanced thermal and dynamic stability of palm fibre-reinforced composites through increased storage modulus and thermal degradation temperature. Moreover, there are a few reports on machining glass fibre-reinforced epoxy composites [28,29].

Traditional methods of material discovery, like the empirical trial-and-error and density functional theory approaches, are facing challenges in keeping pace with the rapidly evolving landscape of materials science. However, the emergence of advanced computational tools, particularly machine learning, has revolutionized material detection, analysis, and design by leveraging robust data processing capabilities

Table 1
Levels of DOE (Taguchi's L_{27} matrix).

Levels	Spindle Speed (RPM)	Feed rate (mm/rev)	Depth of cut (mm)
1	500	0.05	0.3
2	1000	0. 1	0.7
3	1500	0. 15	1.0

Table 2
Details of Taguchi's L_{27}matrix.

Experiment No.	Spindle Speed (RPM)	Feed rate (mm/rev)	Depth of cut (mm)	Experimental Ra (microns)
1	500	0.05	0.3	1.222
2	500	0.05	0.7	1.159
3	500	0.05	1	1.479
4	500	0.1	0.3	1.498
5	500	0.1	0.7	1.509
6	500	0.1	1	1.572
7	500	0.15	0.3	1.773
8	500	0.15	0.7	1.662
9	500	0.15	1	1.599
10	1000	0.05	0.3	0.907
11	1000	0.05	0.7	1.062
12	1000	0.05	1	1.163
13	1000	0.1	0.3	1.248
14	1000	0.1	0.7	1.388
15	1000	0.1	1	1.487
16	1000	0.15	0.3	1.619
17	1000	0.15	0.7	1.712
18	1000	0.15	1	1.766
19	1500	0.05	0.3	0.773
20	1500	0.05	0.7	0.872
21	1500	0.05	1	0.882
22	1500	0.1	0.3	1.219
23	1500	0.1	0.7	1.227
24	1500	0.1	1	1.325
25	1500	0.15	0.3	1.782
26	1500	0.15	0.7	1.882
27	1500	0.15	1	1.856

Table 3
Details of testing data set.

Experiment No.	Spindle Speed(RPM)	Feed rate (mm/rev)	Depth of cut (mm)	Experimental Ra (microns)
1	750	0.06	0.4	0.930
2	900	0.07	0.5	1.092
3	600	0.08	0.6	1.529
4	800	0.09	0.8	1.367
5	1200	0.12	0.9	1.522
6	1300	0.13	0.4	1.822
7	1400	0.11	0.5	1.198
8	1100	0.14	0.9	1.833
9	700	0.09	0.6	1.491

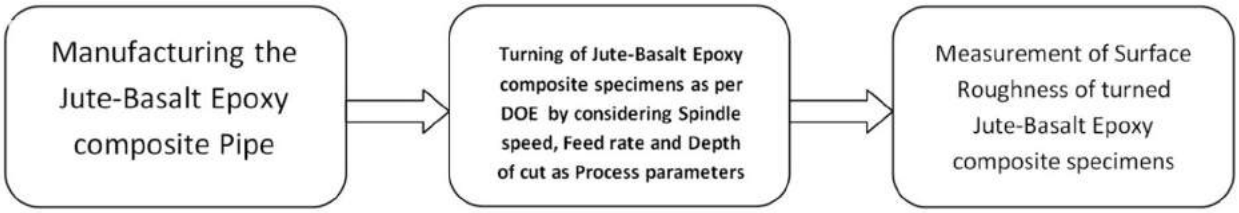

Fig. 1. Schematic represntation of the experimental methodology.

Table 4
Details of GBM model parameters.

Parameter	Details
max_depth	2
n_estimators	3
learning_rate	1.0

Table 5
Details of adaboost model hyperparameters.

Parameter	Details
base_estimator	None
learning_rate	1.0
n_estimators	10,000
random_state	0
loss	linear

and remarkable predictive performance.Machine learning, using boosting techniques like Gradient Boosting Machine (GBM), Adaptive Boosting (AdaBoost), and Extreme Boosting technique (XGBOOST), has demonstrated pervasive effectiveness in various practical applications. Gradient Boosting Machine, a sophisticated machine-learning system, boasts adaptability to specific application demands and different loss functions. Its versatility spans numerous domains. Gradient Boosting Machine has proven pivotal in predicting accidents and collision frequency, particularly considering factors like roadway design, land use, travel demand, disadvantaged neighbourhoods, non-motorized infrastructure, and traffic control [30]. Gradient Boosting Machine is also used to model energy consumption in commercial buildings, and the results showed that it outperformed random forest and linear regression models. Chang et al. used Gradient Boosting Machine to predict PM2.5 concentration change, and their results showed that it surpassed the generalized additive model in terms of prediction accuracy [31,32].

Adaptive Boosting is an iterative approach that continues its convergence until prediction deviations are minimized to their fullest extent, resulting in a robust and accurate model.Across diverse domains, the Adaptive Boosting algorithm has proven adept at boosting prediction accuracy. Examples include predicting component content in rare earth extraction, optimizing demand-driven acquisition, monitoring shield machine posture, and modelling enzyme-small molecule interactions. Notably, in all cases, Adaboost outperformed conventional models [33–36].

XGBOOST, or Extreme Gradient Boosting, is a gradient-based decision tree algorithm that iteratively refines predictions using residuals, continuing until training error is minimized. XGBOOST optimizes leaf node splitting to maximize learning gain.XGBoostpredicted power system inertia, maximum ground settlement, ongoing pregnancy, and lip prominence. The algorithm could find the contributions of every feature towards the performance indicator [37–40].

Surface roughness,a pivotal parameter in epoxy resin characterization, remains inadequately explored, particularly concerning turned jute-basalt epoxy composites. In this study, we aim to investigate the influence of turning process parameters—specifically, the depth of cut, spindle speed, and feed rate on the surface roughness of a novel hybrid composite. This composite is an innovative blend comprising jute fabric, basalt fabric, and various additives.The scarcity of research in this realm underscores the significance of our investigation. By manipulating these turning variables, we seek to elucidate their impact on the surface quality of this unique composite material. To enhance our predictive capabilities, we harnessed advanced machine learning models, including GBM, AdaBoost, and XGBoost, to forecast surface roughness outcomes.

In accordance with the state of art of literaute, it is evident that there are no studies related to the turning operation of Jute Basalt Composites, investigation of effect of turning process parameters on surface roughness of turned Jute-Basalt composites and the corresponding Machine Learning studies. Thus these research gaps are considered as the objectives of this work and the experimental along with numerical findings are presented. The application of Gradient Boosting techniques in the field of machining is also a novelty of this work and so is the contour based experimental validation of aforementioned machibe learning models for the training/testing data sets. The above mentioned Gradient boosting algorithms are used to capture the high non-linearity that exists generally in the data set which cannot be modelled using conventional regression techniques. Our findings unveiled a notable trend: XGBoost exhibited superior predictive performance compared to GBM and AdaBoost. This outcome highlights the efficacy of machine learning techniques in comprehending and modelling the intricate relationships between process parameters and surface roughness in jute-basalt epoxy composites.

2. Experimental

The samples of hybrid Jute-Basalt epoxy composite bars (50 mm outer diameter) required for this work are prepared using jute fabric, basalt fabric, resin (LY556), hardener (HY 905) and catalyst (H-172). Basalt fibreand jute fibre meshes are stacked alternatively by applying the resin in between them until the desired thickness of the composite pipe is achieved. The wrapping of the composite mesh was done on the mandrel, which is mounted on a filament winding machine. The wound fabric is pre-cured in a hot air circulating rotating oven. In this process, the wound fabric and mandrel were heated to a high temperature and then cooled. This pre-curing process took 6 h to get the final composite bar.Jute/basalt epoxy composite specimens were turned using a carbide insert (TNMG 160,408 NN LT 10) on a BFW ORBITUR CNC turning centre. The measurement of surface roughness (Ra) of turned jute/basalt epoxy hybrid composite workpieces was accomplished by the Surfcom Flex 50A machine.

Jute/basalt epoxy composite turning employed Taguchi's L27

Table 6
ANOVA details.

Source	DF	Adj SS	Adj MS	F-Value	P-Value
Regression	3	2.30518	0.76839	43.46	0.000
Spindle Speed	1	0.15217	0.15217	8.61	0.007
Feed Rate	1	2.08897	2.08897	118.16	0.000
Depth of cut	1	0.06404	0.06404	3.62	0.070
Error	23	0.40663	0.01768		
Total	26	2.71181			

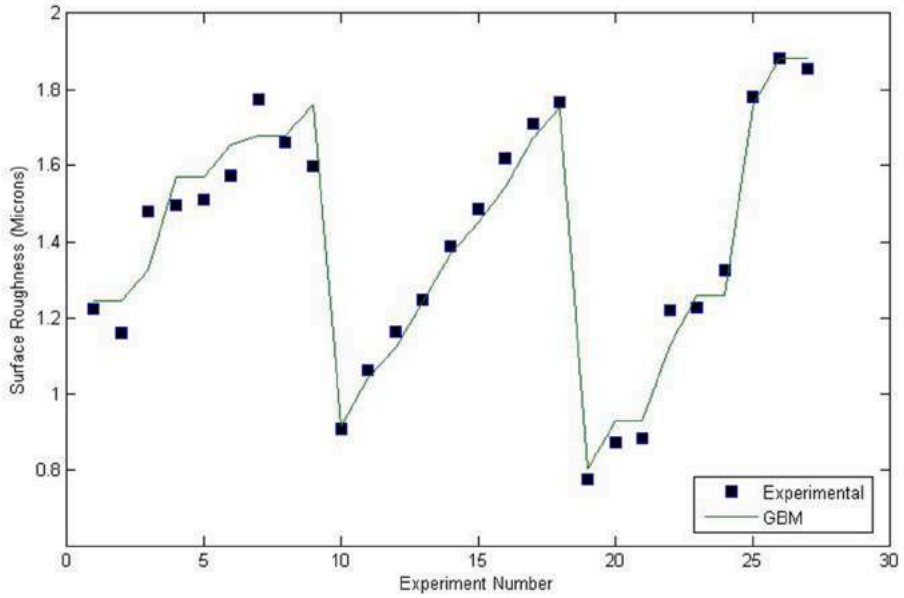

Fig. 2. Comparison plot of GBM and experimentalvalues of Surface Roughness for Training data set.

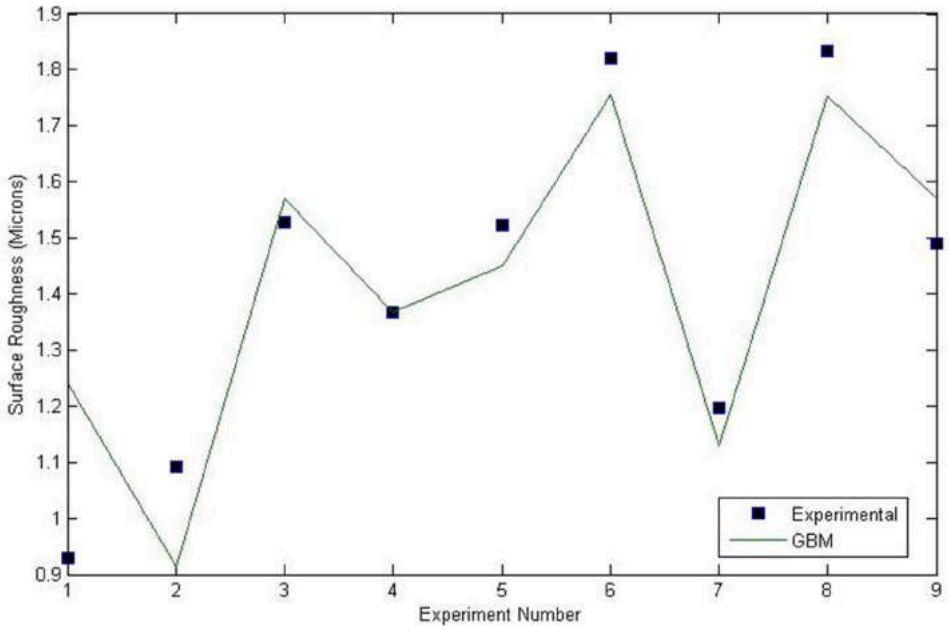

Fig. 3. Comparison plot of GBM and Experimentalvalues of Surface Roughness for Testing data set.

orthogonal array to evaluate the influence of spindle speed, feed rate, and depth of cut. Levels and details of the L27 design are provided in Tables 1 and 2.

The experimental data set, which is required for the validation of machine learning models, is given in Table 3.

The schematic represntation of the experimental methodology adopted in this work is as shown in Fig. 1.

All the machine learning models are trained using the experimental data set as given in Table 2 and the predicted results of all the models are validated with the use of experimental test data set, which is as given in Table 3.

3. Machine learning techniques

Machine learning, a subfield of AI, uses algorithms to learn from data. They mimic the human learning process from which they can make decisions. Machine learning techniques may be unsupervised or supervised, but a supervised learning approach is used in this work. The machine learning models utilized in this work aregradient-boosting techniques such as GBM, Adaboost and XGBoost. The gradient boosting algorithmsare implemented in Jupyter NoteBook through Python scripting.

3.1. Gradient boosting machine (GBM)

Gradient boosting, a powerhouse in machine learning, combines the flexibility of decision trees with the optimization power of iterative gradient descent. It aims to bolster the performance of weak learners by progressively aggregating them, resulting in a robust and powerful learner for classification and prediction tasks. This can be explained

Experimental contour plots

GBM contour plots

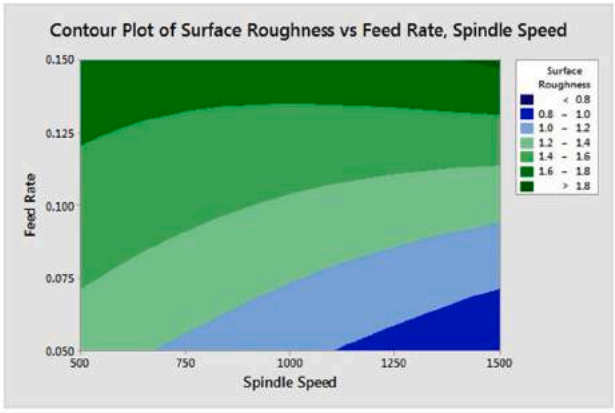

(a)

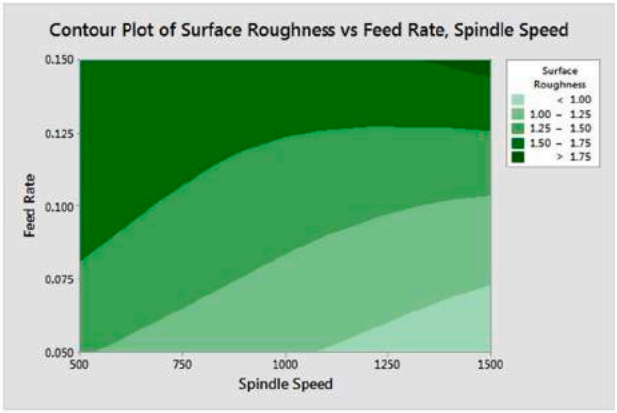

(b)

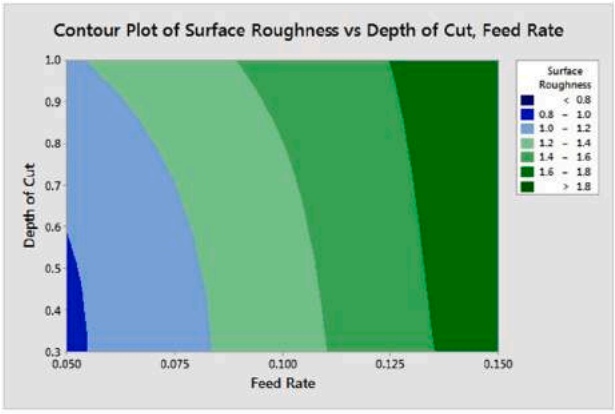

(c)

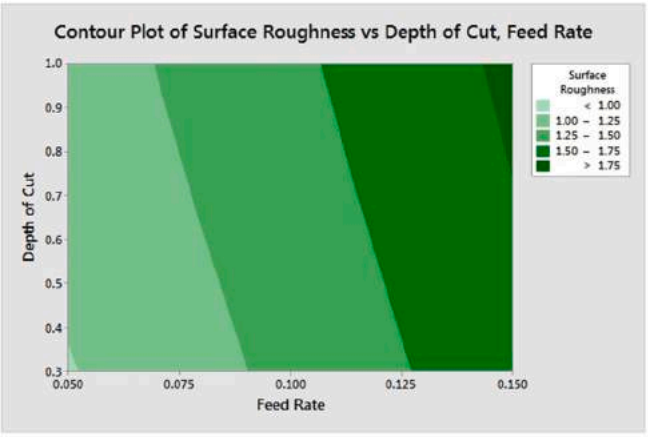

(d)

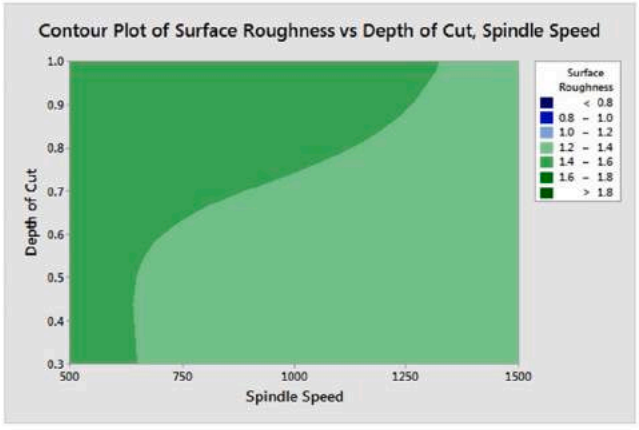

(d)

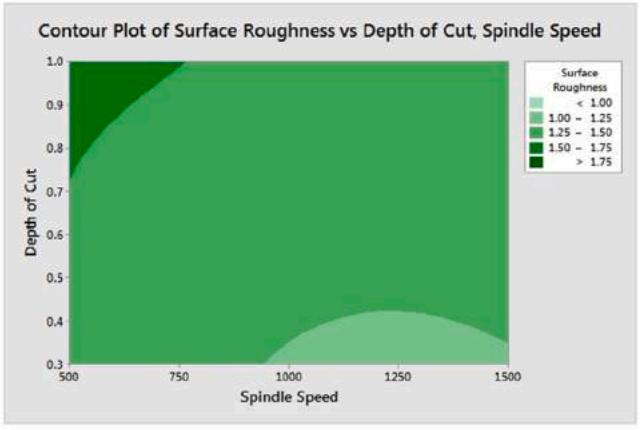

(e)

Fig. 4. Contour plots - GBM (Training Data Set).

Experimental contour plots

GBM contour plots

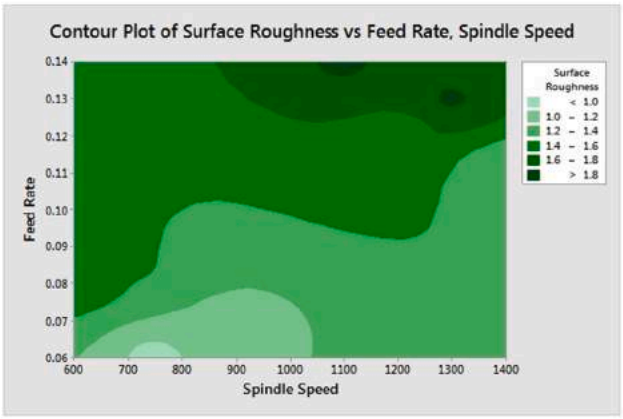

(a)

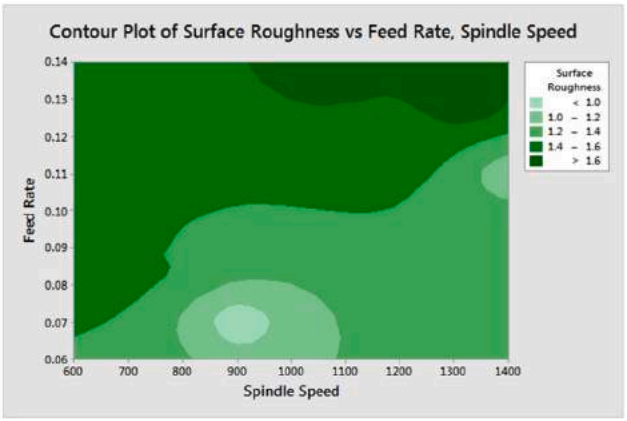

(b)

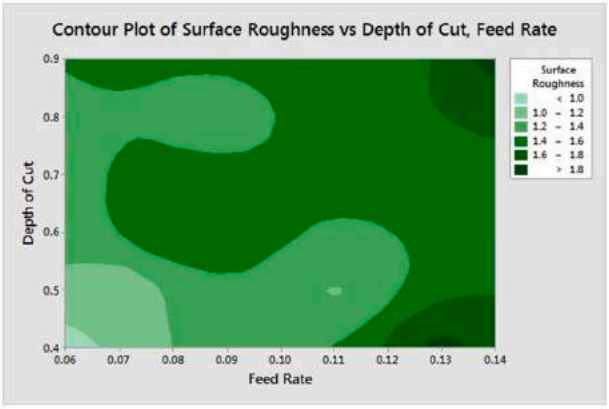

(c)

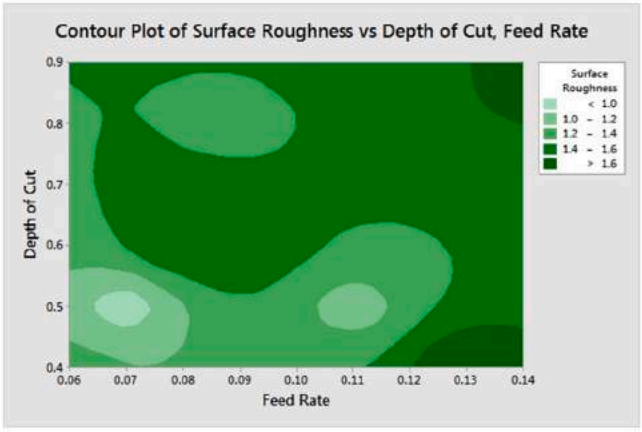

(d)

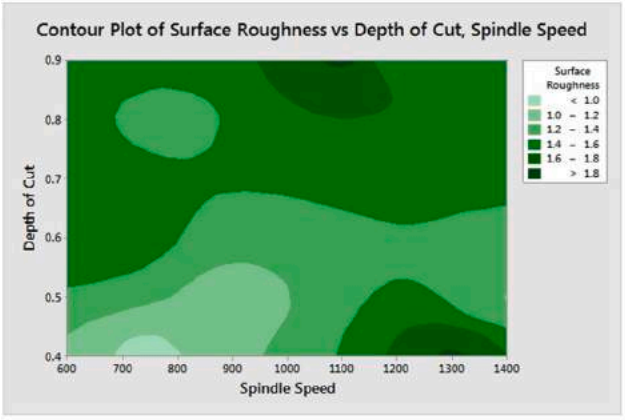

(d)

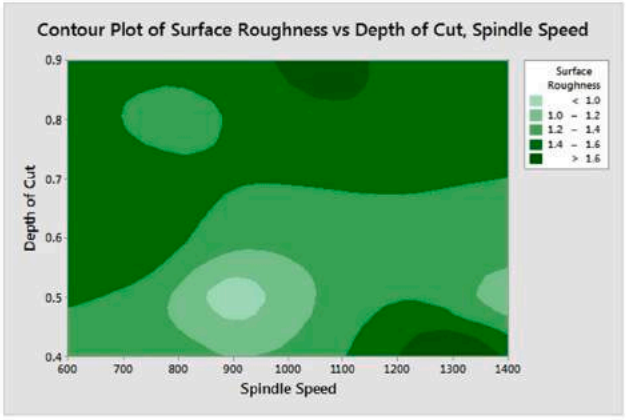

(e)

Fig. 5. Contour plots - GBM (Testing Data Set).

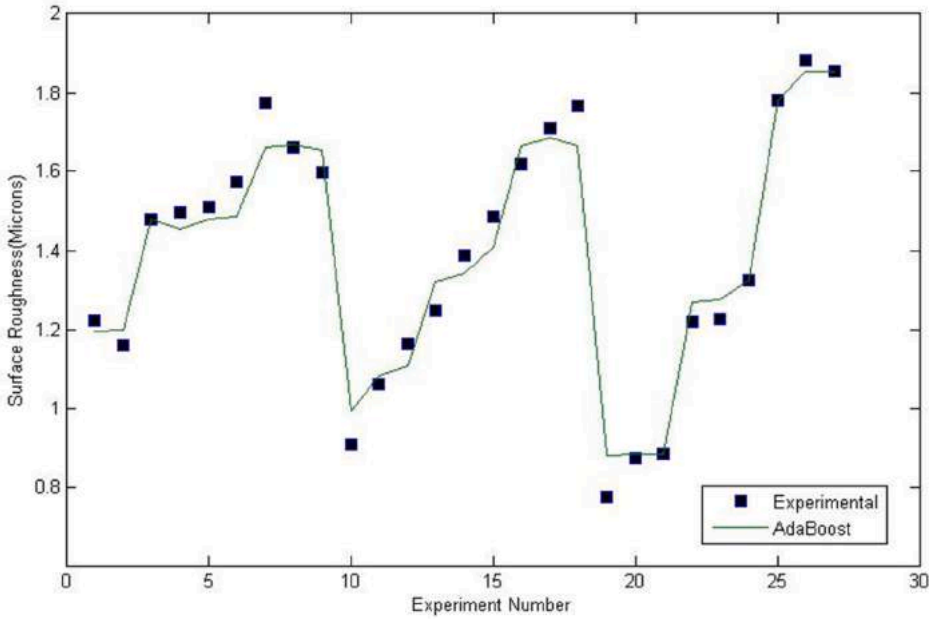

Fig. 6. Comparison plot of AdaBoost and Experimental values of Surface Roughness for Training data set.

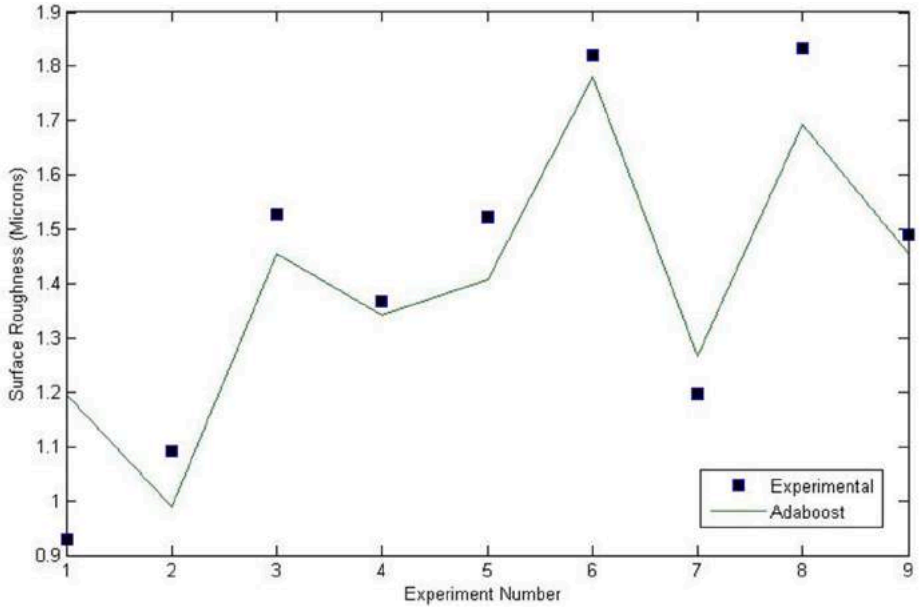

Fig. 7. Comparison plot of AdaBoost and Experimental values of Surface Roughness for Testing data set.

through the set of following equations.

$$A = \varphi(B) \tag{1}$$

The gradient boosting tries to improve the successor $\varphi_{s+1}(B)$ from its predecessor $\varphi_s(B)$

$$\varphi_{s+1}(B) = \varphi_s(B) + h_s(B) \tag{2}$$

where s = number of stages and $h_s(B)$ is residual, which is expressed in Eq. (3)

$$h_s(B) = A - \varphi_s(B) \tag{3}$$

Loss in Mean square error is given by Eq. (4)

$$Loss_{MSE} = \frac{1}{2}(A - \varphi_s(B))^2 \tag{4}$$

The final residual term is expressed by Eq. (5)

$$h_s(B) = -\frac{\partial Loss_{MSE}}{\partial \varphi} = A - \varphi_s(B) \tag{5}$$

The details of the GBM algorithm parametersare given in Table 4.

3.2. Adaptive boosting method

The adaptive boosting technique, most commonly known as AdaBoost, is an ensemble-based machine learning model that converts weak to strong learners. It comprises a series of weak learners through which the data passes sequentially. The succeeding base learners rectify the error associated with the preceding weak learners. This process continues until the predictions' deviations are found to be minimal. The training error is given by Eq. (6)

Experimental contour plots

AdaBoost contour plots

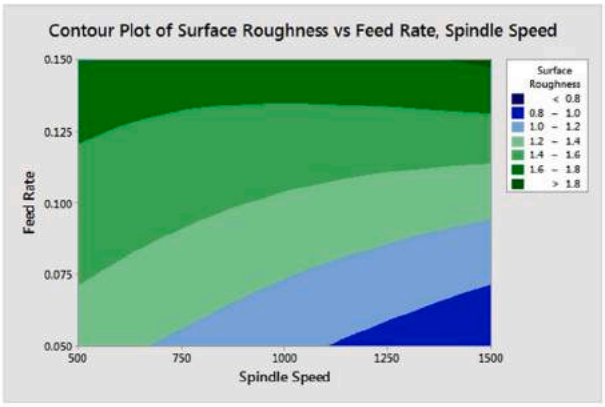

(a)

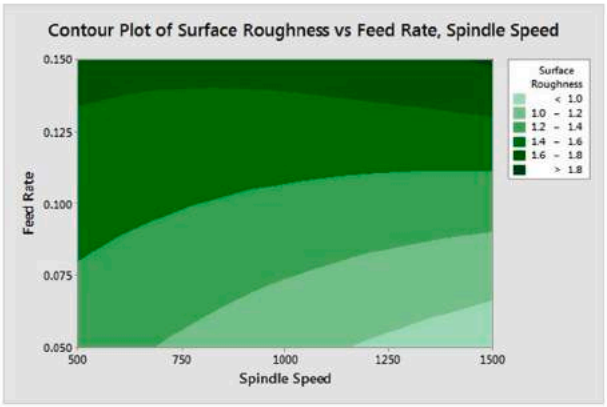

(b)

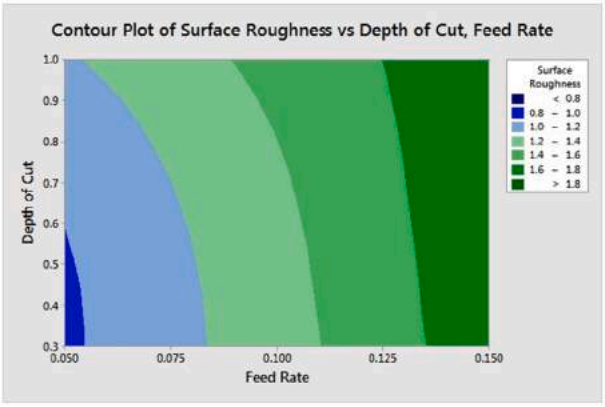

(c)

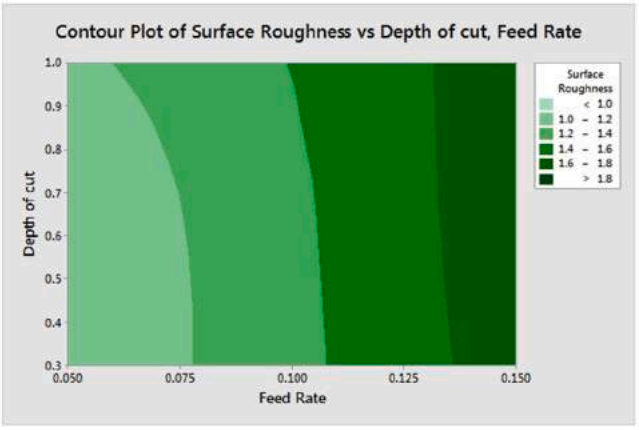

(d)

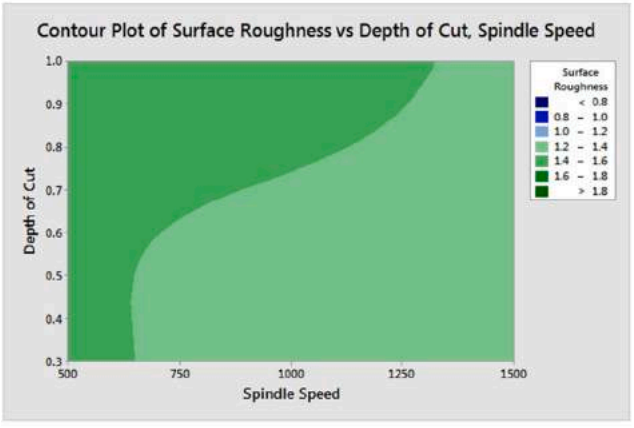

(d)

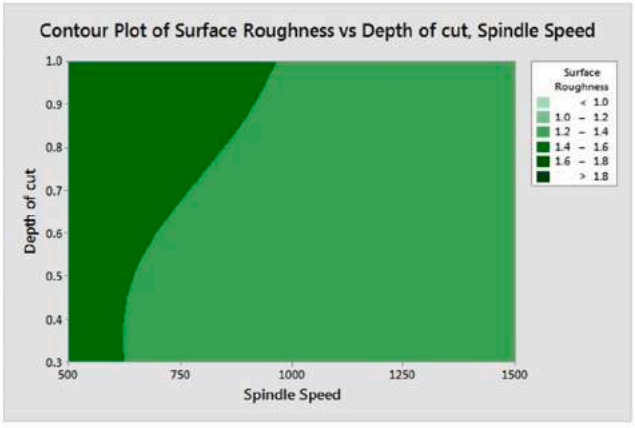

(e)

Fig. 8. Contour plots - AdaBoost (Training Data Set).

Experimental contour plots

GBM contour plots

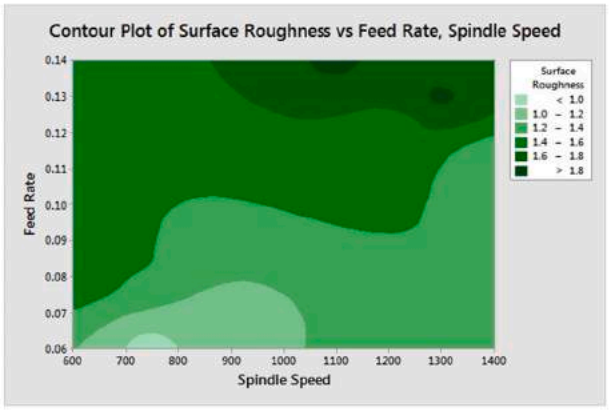

(a)

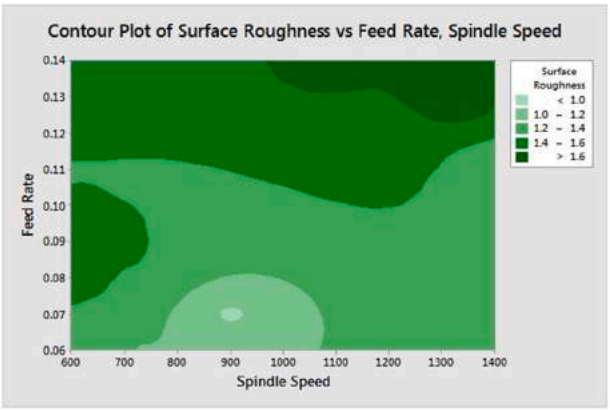

(b)

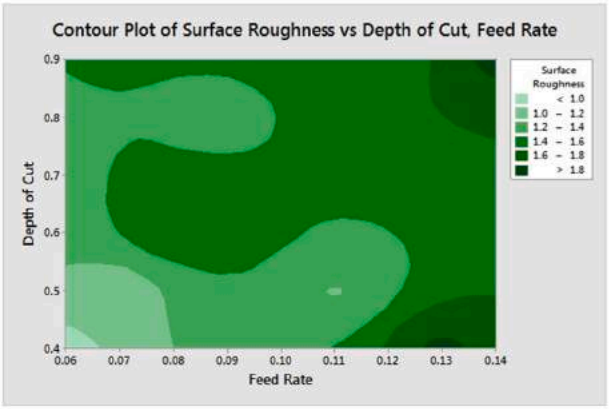

(c)

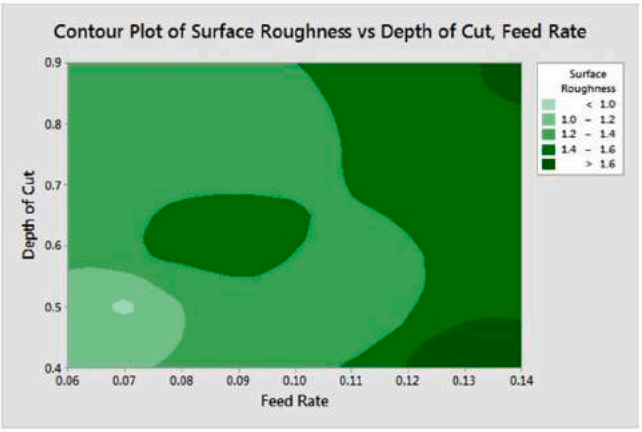

(d)

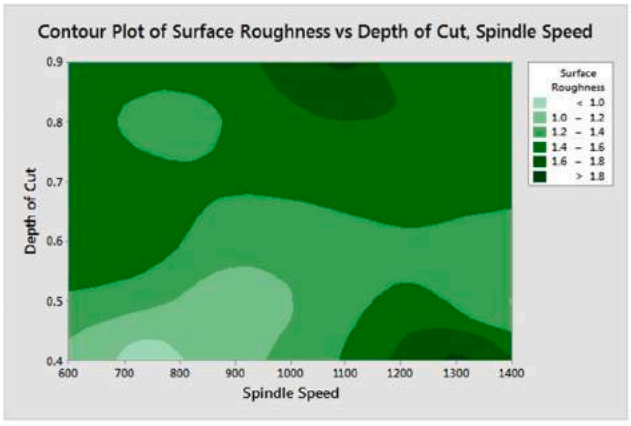

(d)

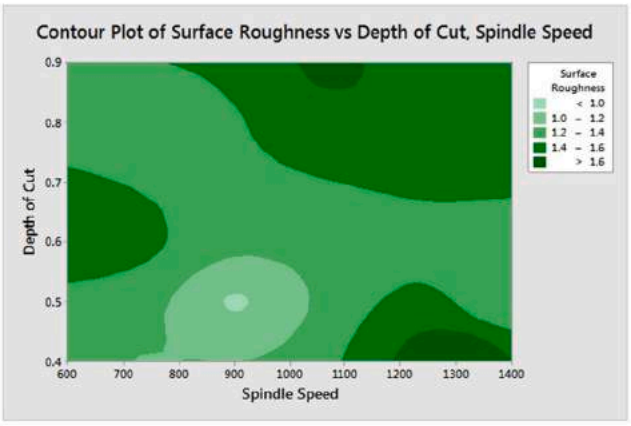

(e)

Fig. 9. Contour plots - AdaBoost (Testing Data Set).

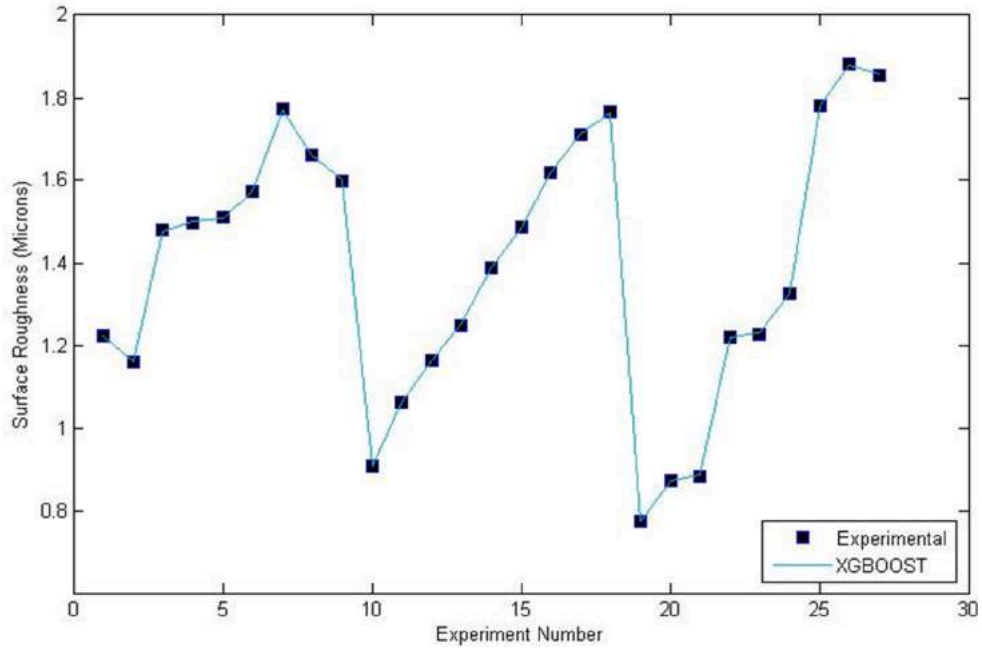

Fig. 10. Comparison plot of XGBOOST and Experimental values of Surface Roughness for Training data set.

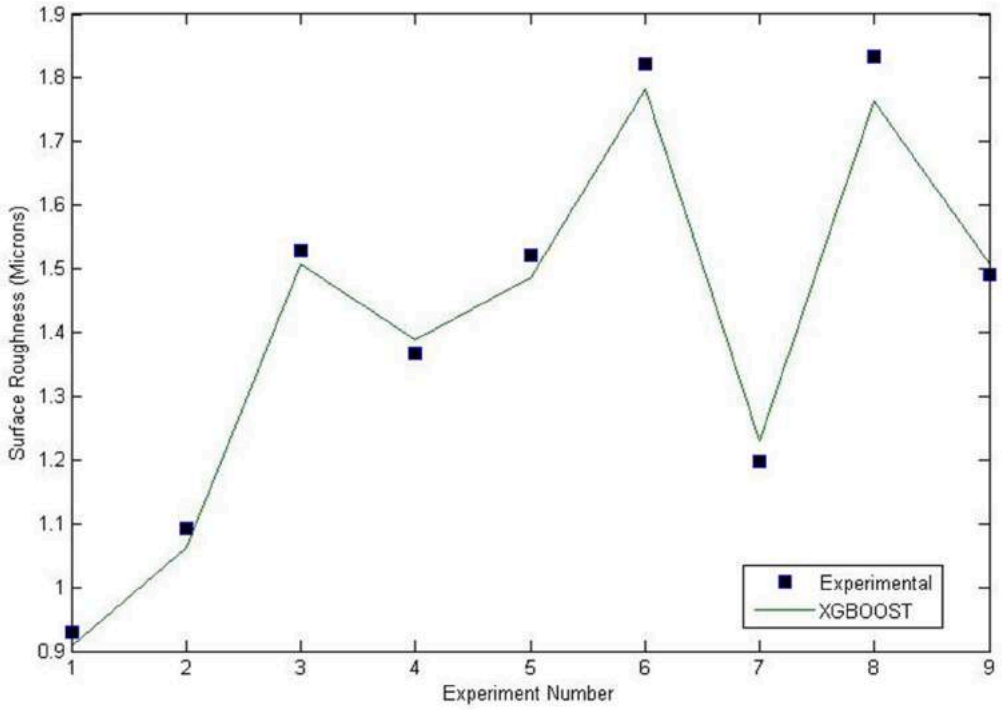

Fig. 11. Comparison plot of XGBOOST and Experimental values of Surface Roughness for Testing data set.

$$E_k = \sum_j E\left[f_{k-1}(z_j) + \alpha_k y(z_j)\right] \quad (6)$$

$E[f_{k-1}]$is the error of trailing learners and$\alpha_k y(z_j)$ is the prediction of a current learner.

The steps involved in building an AdaBoost model are as follows,

1. The dataset is initialized, and equal weights are assigned to every other data point in the data set.
2. The dataset is supplied to the model, and the incorrectly predicted data instances are identified.
3. The weights associated with the incorrectly predicted data instances are increased.
4. If the error is found to be minimum iteration stops; otherwise, steps from 2 to 3 are repeated.

The details of the AdaBoost algorithm parameters are given in Table 5.

Experimental contour plots

XGBOOST contour plots

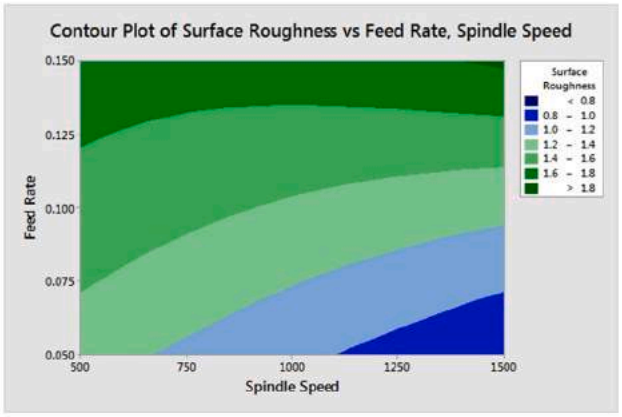

(a)

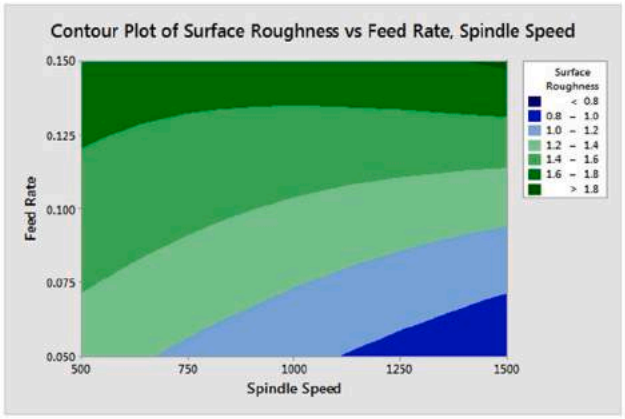

(b)

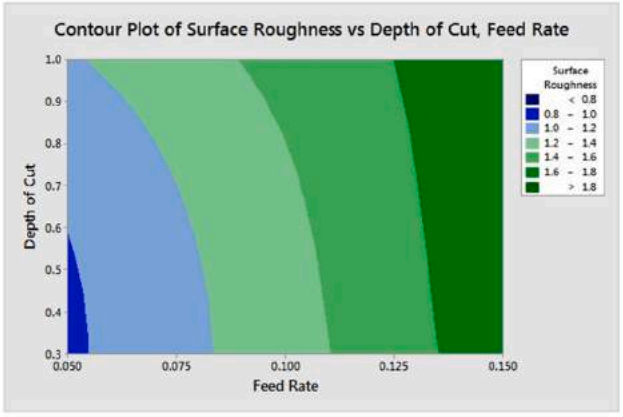

(c)

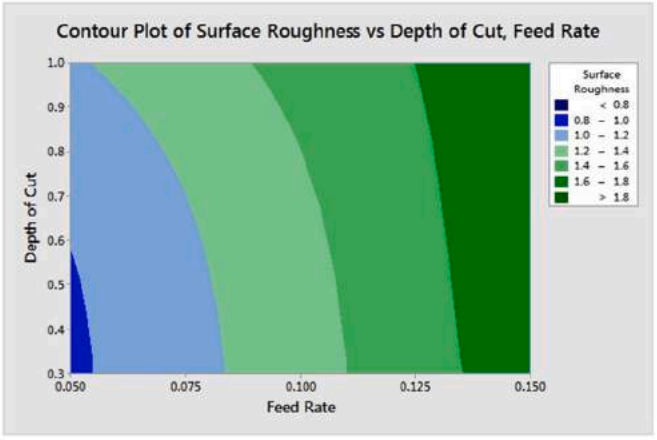

(d)

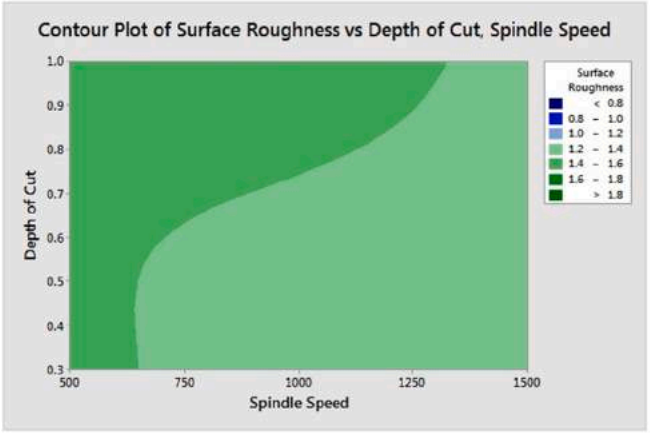

(d)

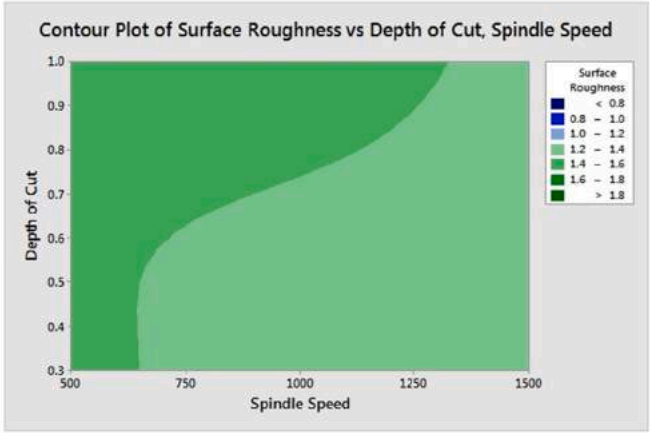

(e)

Fig. 12. Contour plots - XGBOOST (Training Data Set).

Experimental contour plots

GBM contour plots

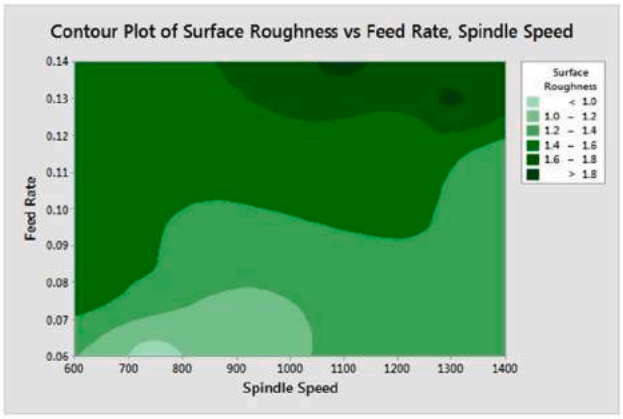

(a)

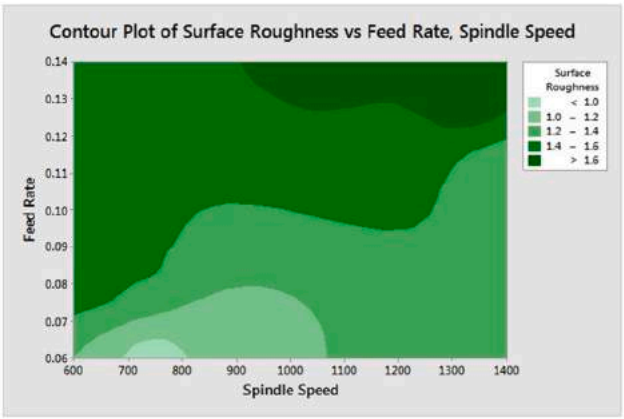

(b)

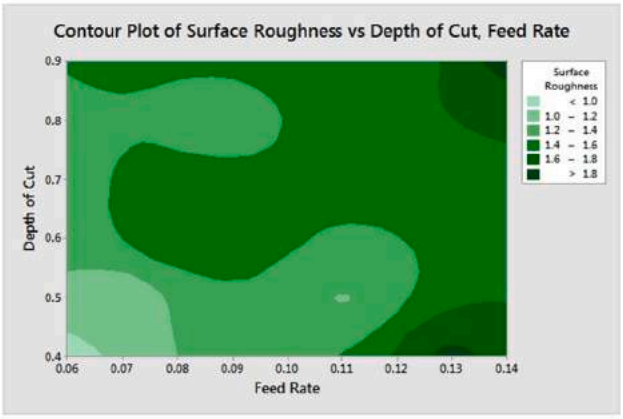

(c)

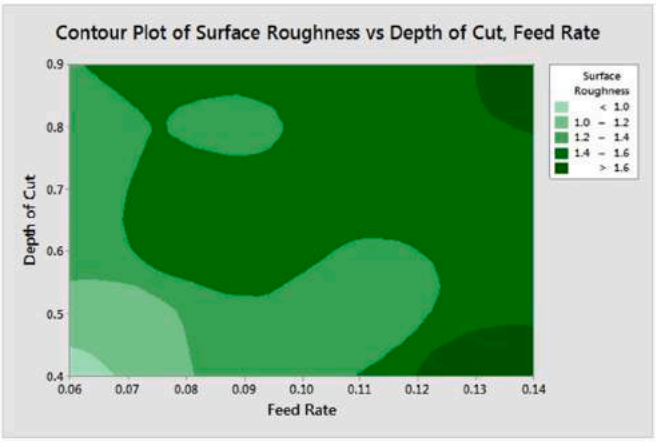

(d)

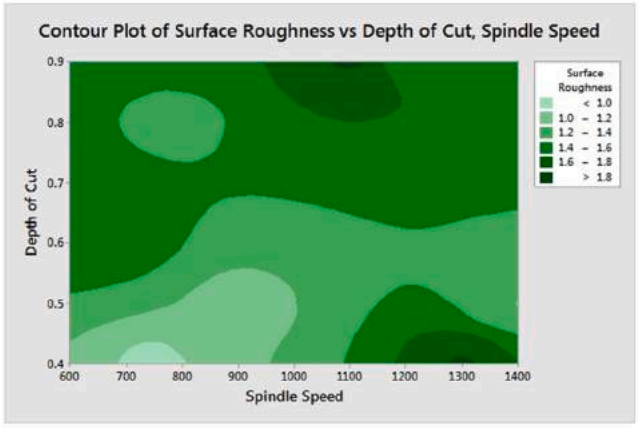

(d)

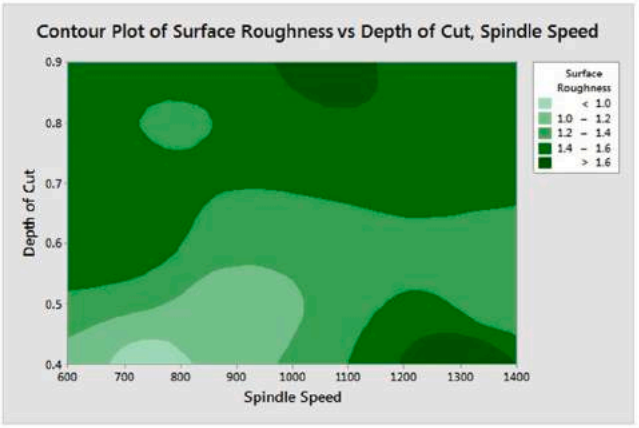

(e)

Fig. 13. Contour plots - XGBOOST (Testing Data Set).

3.3. Extreme gradient boosting method

The extreme gradient boosting method (XGBoost), a widely used gradient-boosting algorithm based on decision trees, excels in machine learning and tries to convert weak learners to strong learners in the algorithm. In this technique, a new learner evolves from the corresponding base learner,utilizingthe residuals of the latter. The algorithm's prediction in each iteration is the sum of the predictions of the current learner and a previous learner. An algorithm like this keeps iterating until the training error becomes minimal. The XGBOOST method adopts the learning strategy to maximize the gain during the leaf node splitting.

The execution of the XGBOOST algorithm includes the growth of the XGBOOST tree and the pruning of each tree. Predictions are then made for each leaf. Following that, further predictions are produced. Finally, the operations are repeated until the loss is low.

The loss function which is needed to be minimized in every iterationis given by Eq. (7),

$$\text{Loss} = \sum_{p=1}^{p=k} l\left(y_p, \varphi_k\left(x_p\right)\right) + \sum_{j=1}^{j=I} L\left(h_j\right) \tag{7}$$

where y_p = output term,x_p = input term, L = regularization factor, h_j = hessian of j^{th} iteration.

4. Results and discussion

The influence of all the turning process parameters,namelyspindle speed, depth of cut, and feed rate, on the surface roughness of machined Jute-Basalt composite specimens are discussed in the section using Analysis of Variance (ANOVA).Many researchers have examined the effect of turning parameters on the Surface roughness of different materials.

Bhardwaj et al. [41]identified spindle speed as the dominant factor affecting surface roughness in EN 353 steel turning, with depth of cut showing minimal impact. They observed decreasing roughness with higher spindle speeds and lower feed rates.Kishore et al. [42].confirm cutting speed as the dominant influence on surface roughness in Al6061-Tic turning. Similar to their findings, we observed minimized roughness with higher spindle speeds and lower feed rates.

Celik and Türkan [43]examined theTurning parameter influence on surface roughness which varied significantly across materials. In chopped glass fibre composites, the feed rate dominates, with minimal impact from the depth of cut. AISI 316 L steel (cermet insert): Feed rate and spindle speed play a critical role in roughness reduction, while the depth of cut remains insignificant. Femoral heads (TiN-Al2O3-TiC tools): Feed rate exerts a strong negative influence, but both speed and depth of cut positively affect roughness. EN-9 steel: Feed rate reigns supreme for surface finish, with the depth of cut and spindle speed having negligible impact. Material-specific optimization is crucial in turning processes. Understanding the unique influence of each parameter on specific materials is vital to achieving the desired surface quality [44–46].Azizi et al. [47]. observed that in both the finish hard turning of AISI 52,100 and AISI H11 tool steel, feed rate emerged as the dominant factor dictating surface roughness, with increasing values directly worsening the finish [48].Aouici et al. [49].,during the turning of X38CrMoV5–1, reported feed rate and cutting speed as surface roughness influencers, with feed rate dominating. Surface finish improved with higher speed and lower feed rate.

A 50 % reduction in surface roughness was achieved by setting all turning parameters (feed rate, spindle speed, and depth of cut) at their minimum levels. This highlights the importance of material-specific optimization for Ti-6Al-4 V, as the effect of parameters on surface finish varies significantly across materials. In the present work, the Analysis of variance (ANOVA) is carried out using MINITAB 17 statistical software. ANOVA from Table 6 pinpoints feed rate and spindle speed as significant influences on surface roughness ($p < 0.05$), while the depth of cut shows negligible impact. This implies optimizing feed rate and spindle speed optimization to minimize surface roughness in Ti-6Al-4 V components. Optimizing turning parameters for Ti-6Al-4 V is crucial for achieving desired surface finishes, ultimately impacting component performance and lifespan. This study emphasizes the importance of focusing on feed rate and spindle speed when aiming for minimal surface roughness in turned Ti-6Al-4 V parts [50].

The GBM model predicted surface roughness values of turned jute/basalt composites and the experimental values for training and testing data set, plotted in Figures2 and 3, respectively.

The GBM-predicted values of Surface Roughness for Trainingand Testing data sets are plotted in Fig.2 and Fig.3, respectively. The average and maximum error of GBM predicted values of Surface Roughness for the Training data setare 0.051 μm and 0.161microns, respectively. In contrast, the respective values for the testing data set are 0.10microns and 0.31microns, respectively.

The contours of the GBM model predicted, and experimental values for the training and testing data set are plotted in Figs. 4 and5, respectively.

Table 7
Statistical ranking table.

Level	Spindle Speed (RPM)	Feed rate (mm/rev)	Depth of cut (mm)
1	1.497	1.058	1.338
2	1.372	1.386	1.386
3	1.313	1.739	1.459
Delta	0.184	0.681	0.121
Rank	2	1	3

Table 8
Details of turning process parameters for minimum surface roughness in different composite materials.

Material	Minimum Surface Roughness (μm)	Process Parameters			Reference
		Speed	Feed Rate mm/rev	Depth of Cut (mm)	
GFRP composites with graphite/fly ash	0.316	50 m/min	0.1	0.5	[51]
Macro Banana fibre Reinforced Epoxy Composites	2.514	300 RPM	0.1	1	[52]
Micro Banana fibre Reinforced Epoxy Composites	3.282	450 RPM	0.1	2	[52]
Short Banana fibre Reinforced Epoxy Composites	2.577	300 RPM	0.1	1	[52]
Glass epoxy Composites	3.79	100 m/min	0.05	0.5	[53]
Carbon fibre Reinforced Polymer Composites	1.11	100 m/min	0.05	0. 15	[54]
Banana fibre and Silicon Carbide Reinforced Polymer Matrix Composites	1.809	500 RPJ	0.15	0.4	[55]
Nylon 6 Composite	0.26	1400 rpm	0.05	0.2	[56]
Jute Basalt composite	0.773	1500 rpm	0.05	0.3	Present work

Fig. 4 and Fig.5 show that there are many mismatches between the experimental and GBM contours of Surface Roughness.The AdaBoost model predicted surface roughness values of turned Jute/Basalt composites, along with the experimental values for training and testing data sets are plotted in Fig.6 and Fig.7, respectively.

The average and maximum error of AdaBoost's predicted roughness values for the training data setis 0.043 μm and 0.111 μm, respectively. In contrast, for the testing data set, the respective values are 0.096 μm and 0.266 μm, respectively.

The surface roughness contours of the AdaBoost model predicted values, along with the experimental values for the training and testing data set, are plotted in Fig.8 and Fig.9, respectively.

From Fig. 8 and Fig.9, it can be seen that there is a little mismatch between the experimental and AdaBoost contours of surface roughness.

The XGBOOST model predicted surface roughness values of turned Jute/Basalt composites, and the experimental values for training and testing data set are plotted in Fig.10 and Fig.11, respectively.

The average and maximum error of XGBOOST's predicted roughness values for the training data setis 0.001 μm and 0.005 μm, respectively. In contrast, for the testing data set, the respective values are 0.032 μm and 0.069 μm, respectively.

The Contours of the XGBOOST model predicted values and the experimental values for the training and testing data set are plotted in Fig.12 and Fig.13, respectively.

It is evident From Fig.12 and Fig. 13 that there is an exact match between the experimental and XGBOOST contours of Surface Roughness. The reason for this exact match of XGboost as compared to Adaboost and GBM is because of its handling capability of missing values in the data set, better generalizarion due to the built-in regularization process use of advanced optimization techniques and more efficient capturing of complex patterns in the data set.

The main effects plot from Figure 14 (Supplementary material) depicts the fact of an increase of Surface roughness with the increase of depth of cut and Feed rate. However, the surface roughness decreased with the rise in Spindle speed.

The percentage error in surface roughness prediction for all the machine learning models is calculated by Eq. (8),

$$\text{Percentage Error in Prediction } = \frac{(\textit{PredictedRoughness Value} - \textit{Experimental Roughness Value}) \times 100}{\textit{Experimental Roughness Value}} \tag{8}$$

According to Figure 15 (a) (Supplementary material), the Mean absolute percentage error for the training data set of GBM, AdaBoost and XGBOOST Machine learning models are 3.75 %, 3.36 % and 0.11 %, respectively. For the testing data set, themean absolute percentage errors of GBM, AdaBoost, and XGBOOST are found to be 8.50 %, 7.81 %, and 2.24 %, respectively, from Figure 15 (b). It is observed from Figure 16 (a) (Supplementary material) that the maximum percentage errors of GBM, AdaBoost and XGBOOST are 10.41 %, 13.86 % and 0.33 % for the case of the training data set from Figure 16 (b) (Supplementary material). Maximum percentage errors are 33.58 %, 28.62 % and 3.78 % for GBM, AdaBoost and XGBOOST models for the testing data instances. Looking into the maximum and average prediction errors, XGBOOST performs better than others. The feature importance of the XGBOOST model is computed, which is given in Figure 17 (Supplementary material). According to the feature importance plot, the ranking order of the influencing process parameters is feed followed by spindle speed and depth of cut, which is also true according to the Minitab computed delta ranking table, whose details are given in Table 7.

The details of the minimum Surface Roughness Values obtained while turning the different epoxy-based composite specimens are given in Table 8.

5. Conclusions

Integrating basalt fibres into jute fibre composites presents a promising avenue for lightweight and cost-efficient solutions in various industries. This study delved into the fabrication of jute/basalt epoxy composite bars and the subsequent investigation of turning process parameters depth of cut, feed rate, and spindle speed on the surface roughness of the resulting specimens. The insights drawn from this investigation have yielded significant conclusions:

ANOVA results underscore the substantial impact of feed rate and spindle speed on surface roughness, while the depth of cut exhibits insignificance.The experimental results suggest that increasing spindle speed and decreasing both feed rate and depth of cut correspond to reduced surface roughness in turned specimens.According to Taguchi's orthogonal matrix, the minimum surface roughness was obtained when the spindle speed, feed rate and depth of cut were 1500 RPM, 0.05 mm/rev and 0.3 mm, respectively. The minimum surface roughness values for the experimental, GBM, AdaBoost, and XGBoost cases are found to be 0.773 μm, 0.800 μm, 0.880 μm, and 0.774 μm, respectively.By Machine Learning Insights: Leveraging the feature importance aspect of machine learning models has allowed us to ascertain the hierarchy of process variables influencing the performance indicator,establish that feed rate exhibits the highest influence, followed by spindle speed and depth of cut, recognize XGBoost's notable superiority in predictive accuracy over GBM and AdaBoos and validate the precision of XGBoost's Surface Roughness contours, which closely align with experimental contours across training and testing datasets.These findings underscore the pivotal role of process parameters in influencing the surface quality of jute/basalt epoxy composites, emphasizing the potential of machine learning in predicting and optimizing material properties in manufacturing processes.

CRediT authorship contribution statement

Amith Gadagi: Investigation, Formal analysis. **Baskaran Sivaprakash:** Investigation. **Chandrashekar Adake:** Formal analysis. **Umesh Deshannavar:** Visualization, Validation, Investigation. **Prasad G. Hegde:** Software, Formal analysis. **Santhosh P.:** Writing – review & editing, Writing – original draft, Validation, Software, Project administration, Methodology, Investigation, Formal analysis, Data curation, Conceptualization. **Natarajan Rajamohan:** Writing – review & editing, Validation, Software, Methodology, Investigation, Data curation, Conceptualization. **Ahmed I. Osman:** Writing – review & editing.

Declaration of competing interest

The authors declare that they have no known competing financial interests or personal relationships that could have appeared to influence the work reported in this paper.

Data availability

The authors do not have permission to share data.

Supplementary materials

Supplementary material associated with this article can be found, in the online version, at doi:10.1016/j.jcomc.2024.100453.

References

[1] M.R. Sanjay, P. Madhu, M. Jawaid, P. Senthamaraikannan, S. Senthil, S. Pradeep, Characterization and properties of natural fiber polymer composites: a comprehensive review, J. Clean. Prod. 172 (2018) 566–581, https://doi.org/10.1016/j.jclepro.2017.10.101.

[2] T. Hojo, Z. Xu, Y. Yang, H. Hamada, Tensile Properties of Bamboo, Jute and Kenaf Mat-reinforced Composite. Energy Procedia 56 (2014) 72–79, https://doi.org/10.1016/j.egypro.2014.07.133.

[3] H. Alshahrani, T.A. Sebaey, M.M. Awd Allah, M.A Abd El-baky, Jute-basalt reinforced epoxy hybrid composites for lightweight structural automotive applications, J. Compos. Mater. 57 (2023) 1315–1330, https://doi.org/10.1177/00219983231155013.

[4] G. Santosh Gangappa, S. Sripad Kulkarni, Experimentation and validation of basalt & jute fiber reinforced in polymer matrix hybrid composites, Mater. Today Proc. 38 (2021) 2372–2379, https://doi.org/10.1016/j.matpr.2020.07.081.

[5] M. Kishore, M. Amrita, Mechanical characterization of jute-basalt hybrid composites with graphene as nanofiller, J. Mech. Sci. Technol. 36 (2022) 3923–3929, https://doi.org/10.1007/s12206-022-0714-5.

[6] S. D, T Krishnamurthy, An investigation of basalt/E-glass hybrid composite pipe on drilling using Box–Behnken design, Mater. Manuf. Process 38 (2023) 1104–1118, https://doi.org/10.1080/10426914.2023.2165667.

[7] R. Ganesh, P. Anand, Experimental investigation on mechanical properties of Basalt/Jute/SiC reinforced hybrid polymer composites, Mater. Today Proc. 59 (2022) 1636–1642, https://doi.org/10.1016/j.matpr.2022.03.327.

[8] M. Kishore, M. Amrita, B. Kamesh, Experimental investigation of milling on basalt-jute hybrid composites with graphene as nanofiller, Mater. Today Proc. 43 (2021) 726–730, https://doi.org/10.1016/j.matpr.2020.12.847.

[9] Y.H. Çelik, E. Kilickap, A.İ. Kilickap, An experimental study on milling of natural fiber (jute)- reinforced polymer composites, J. Compos. Mater. 53 (2019) 3127–3137, https://doi.org/10.1177/0021998319826373.

[10] T. Premkumar, S. Irulappasamy, S. Rajesh, J.T.W. Jappes, S.C. Amico, Investigation to Appraise the Abrasive Water Jet Response of Curaua/Basalt Hybrid Polyester Composites, Int. J. Manuf. Mater. Mech. Eng. 9 (2019) 13–29, https://doi.org/10.4018/IJMMME.2019010102.

[11] Y.H. Çelik, M.S. Alp, Determination of Milling Performance of Jute and Flax Fiber Reinforced Composites, J. Nat. Fibers 19 (2022) 782–796, https://doi.org/10.1080/15440478.2020.1764435.

[12] A. Rajendran, B. Paul, K. Shunmugesh, Optimization of milling parameters in jute fiber reinforced epoxy composite using GRA, Mater. Today Proc. 43 (2021) 3951–3955, https://doi.org/10.1016/j.matpr.2021.02.663.

[13] S.R. Madara, R.N.S. Sarath, J.T. Varghese, C. Pon Selvan, Experimental Investigations on Abrasive Waterjet Machining of Hybridized Kevlar With Jute Fiber Reinforced Epoxy Composite Using Taguchi & ANOVA Approach, in: 2019 Adv. Sci. Eng. Technol. Int. Conf, IEEE, 2019, pp. 1–9, https://doi.org/10.1109/ICASET.2019.8714323.

[14] V. Sridharan, M. Nambi, S. Deivanayagam, Comparison of Machinability of Glass/Jute Fabric Polymer Composites, Appl. Mech. Mater. 440 (2013) 42–46, https://doi.org/10.4028/www.scientific.net/AMM.440.42.

[15] A. Jain, B. Singh, K. Sharma, Y. Shrivastava, Fabrication, Testing and Machining of Hybrid Basalt-Glass Fiber Reinforced Plastic composite, Indian J. Pure Appl. Phys. 59 (2021) 258–262.

[16] A. Harun, C.H Che Haron, J. Ghani, S. Mokhtar, S Ting, Study the effect of milling parameters on surface roughness during milling Kenaf fibre reinforced plastic, Adv. Environ. Biol. 9 (2015) 46. +.

[17] R. Vinayagamoorthy, N. Rajeswari, S. Sivanarasimha, K. Balasubramanian, Fuzzy Based Optimization of Thrust Force and Torque during Drilling of Natural Hybrid Composites, Appl. Mech. Mater. 787 (2015) 265–269, https://doi.org/10.4028/www.scientific.net/AMM.787.265.

[18] M. Ramesh, K. Palanikumar, K.H. Reddy, Influence of Tool Materials on Thrust Force and Delamination in Drilling Sisal-glass Fiber Reinforced Polymer (S-GFRP) Composites, Procedia Mater. Sci. 5 (2014) 1915–1921, https://doi.org/10.1016/j.mspro.2014.07.513.

[19] S.A.S. Azuan, J.M. Juraidi, W.M.W. Muhamad, Evaluation of Delamination in Drilling Rice Husk Reinforced Polyester Composites, Appl. Mech. Mater. 232 (2012) 106–110, https://doi.org/10.4028/www.scientific.net/AMM.232.106.

[20] M. Sakthivel, S. Vijayakumar, N.K. Prasad, Drilling analysis on basalt/sisal reinforced polymer composites using ANOVA and regression model, Appl. Math. Sci. 9 (2015) 3285–3290, https://doi.org/10.12988/ams.2015.54315.

[21] S. Jayabal, U. Natarajan, U. Sekar, Regression modeling and optimization of machinability behavior of glass-coir-polyester hybrid composite using factorial design methodology, Int. J. Adv. Manuf. Technol. 55 (2011) 263–273, https://doi.org/10.1007/s00170-010-3030-7.

[22] S. Jayabal, U. Natarajan, Drilling analysis of coir-fibre-reinforced polyester composites, Bull. Mater. Sci. 34 (2011) 1563–1567, https://doi.org/10.1007/s12034-011-0359-y.

[23] K. Debnath, I. Singh, A. Dvivedi, Drilling Characteristics of Sisal Fiber-Reinforced Epoxy and Polypropylene Composites, Mater. Manuf. Process 29 (2014) 1401–1409, https://doi.org/10.1080/10426914.2014.941870.

[24] F.M. AL-Oqla, M.A. Omari, A Al-Ghraibah, Predicting the potential of biomass-based composites for sustainable automotive industry using a decision-making model. Lignocellul. Fibre Biomass-Based Compos. Mater, Elsevier, 2017, pp. 27–43, https://doi.org/10.1016/B978-0-08-100959-8.00003-2.

[25] A. Haque, D. Mondal, I. Khan, M.A. Usmani, A.H. Bhat, U. Gazal, Fabrication of composites reinforced with lignocellulosic materials from agricultural biomass. Lignocellul. Fibre Biomass-Based Compos. Mater, Elsevier, 2017, pp. 179–191, https://doi.org/10.1016/B978-0-08-100959-8.00010-X.

[26] A. Shahzad, Mechanical properties of lignocellulosic fiber composites. Lignocellul. Fibre Biomass-Based Compos. Mater, Elsevier, 2017, pp. 193–223, https://doi.org/10.1016/B978-0-08-100959-8.00011-1.

[27] N. Saba, M. Jawaid, M.T.H. Sultan, Thermal properties of oil palm biomass based composites. Lignocellul. Fibre Biomass-Based Compos. Mater, Elsevier, 2017, pp. 95–122, https://doi.org/10.1016/B978-0-08-100959-8.00006-8.

[28] A. Gadagi, C. Adake, A constrained multi-objective optimization of turning process parameters by genetic algorithm and particle swarm optimization techniques, Mater. Today Proc. 42 (2021) 1207–1212, https://doi.org/10.1016/j.matpr.2020.12.692.

[29] A. Gadagi, C. Adake, Radial basis artificial neural network assisted multiple regression analysis of a GFRP turned composites, Mater. Today Proc. 42 (2021) 1213–1217, https://doi.org/10.1016/j.matpr.2020.12.695.

[30] R. An, Z. Tong, Y. Ding, B. Tan, Z. Wu, Q. Xiong, et al., Examining non-linear built environment effects on injurious traffic collisions: a gradient boosting decision tree analysis, J. Transp. Heal. 24 (2022) 101296, https://doi.org/10.1016/j.jth.2021.101296.

[31] S. Touzani, J. Granderson, S. Fernandes, Gradient boosting machine for modeling the energy consumption of commercial buildings, Energy Build. 158 (2018) 1533–1543, https://doi.org/10.1016/j.enbuild.2017.11.039.

[32] B. Cheng, Y. Ma, F. Feng, Y. Zhang, J. Shen, H. Wang, et al., Influence of weather and air pollution on concentration change of PM2.5 using a generalized additive model and gradient boosting machine, Atmos. Environ. 255 (2021) 118437, https://doi.org/10.1016/j.atmosenv.2021.118437.

[33] Y. Hui, L. Shuli, L. Rongxiu, Z. Jianyong, Prediction of component content in rare earth extraction process based on ESNs-Adaboost, IFAC-PapersOnLine 51 (2018) 42–47, https://doi.org/10.1016/j.ifacol.2018.09.390.

[34] K.W. Walker, Z. Jiang, Application of adaptive boosting (AdaBoost) in demand-driven acquisition (DDA) prediction: a machine-learning approach, J. Acad. Librariansh 45 (2019) 203–212, https://doi.org/10.1016/j.acalib.2019.02.013.

[35] H. Xiao, Z. Chen, R. Cao, Y. Cao, L. Zhao, Y. Zhao, Prediction of shield machine posture using the GRU algorithm with adaptive boosting: a case study of Chengdu Subway project, Transp Geotech 37 (2022) 100837, https://doi.org/10.1016/j.trgeo.2022.100837.

[36] B. Niu, Y. Jin, L. Lu, K. Fen, L. Gu, Z. He, et al., Prediction of interaction between small molecule and enzyme using AdaBoost, Mol. Divers. 13 (2009) 313–320, https://doi.org/10.1007/s11030-009-9116-1.

[37] L. Zhang, Z. Guo, Q. Tao, Z. Xiong, J. Ye, XGBoost-based short-term prediction method for power system inertia and its interpretability, Energy Reports 9 (2023) 1458–1469, https://doi.org/10.1016/j.egyr.2023.04.065.

[38] J. Su, Y. Wang, X. Niu, S. Sha, J. Yu, Prediction of ground surface settlement by shield tunneling using XGBoost and Bayesian Optimization, Eng. Appl. Artif. Intell. 114 (2022) 105020, https://doi.org/10.1016/j.engappai.2022.105020.

[39] Y. Li, H. Duan, S. Wang, An XGBoost predictive model of ongoing pregnancy in patients following hysteroscopic adhesiolysis, Reprod. Biomed. Online 46 (2023) 965–972, https://doi.org/10.1016/j.rbmo.2023.01.019.

[40] L. Xing, X. Zhang, Y. Guo, D. Bai, H. Xu, XGBoost-aided prediction of lip prominence based on hard-tissue measurements and demographic characteristics in an Asian population, Am J. Orthod Dentofac Orthop (2023), https://doi.org/10.1016/j.ajodo.2023.01.017.

[41] B. Bhardwaj, R. Kumar, P.K. Singh, Prediction of Surface Roughness in Turning of EN 353 Using Response Surface Methodology, Trans. Indian Inst. Met. 67 (2014) 305–313, https://doi.org/10.1007/s12666-013-0346-7.

[42] D.S.C. Kishore, K.P. Rao, S.M.J. Basha, B.J.P. Rao, Investigation Of Surface Roughness In Turning of In-situ Al6061-TiC Metal Matrix Composite By Taguchi And Prediction Of Response by ANN, Mater. Today Proc. 5 (2018) 18070–18079, https://doi.org/10.1016/j.matpr.2018.06.141.

[43] Y.H. Çelik, C. Türkan, Investigation of mechanical characteristics of GFRP composites produced from chopped glass fiber and application of taguchi methods to turning operations, SN. Appl. Sci. 2 (2020) 849, https://doi.org/10.1007/s42452-020-2684-5.

[44] Y. Touggui, S. Belhadi, S.-E. Mechraoui, A. Uysal, M.A. Yallese, M. Temmar, Multi-objective optimization of turning parameters for targeting surface roughness and maximizing material removal rate in dry turning of AISI 316L with PVD-coated cermet insert, SN. Appl. Sci. 2 (2020) 1360, https://doi.org/10.1007/s42452-020-3167-4.

[45] N.I. Galanis, D.E. Manolakos, Surface roughness prediction in turning of femoral head, Int. J. Adv. Manuf. Technol. 51 (2010) 79–86, https://doi.org/10.1007/s00170-010-2616-4.

[46] Khurshid S., Zainab M., Farooq Y., Yousuf F., Ayoub T., Mir F.A., et al. Effect of Turning Parameters on Surface Roughness of EN-9 Steel Using Taguchi Robust design—An Analysis, 2022, p. 203–11. https://doi.org/10.1007/978-981-16-4222-7_24.

[47] M.W. Azizi, S. Belhadi, M.A. Yallese, T. Mabrouki, J.-F. Rigal, Surface roughness and cutting forces modeling for optimization of machining condition in finish hard turning of AISI 52100 steel, J. Mech. Sci. Technol. 26 (2012) 4105–4114, https://doi.org/10.1007/s12206-012-0885-6.

[48] S. Saini, I.S. Ahuja, V.S. Sharma, Influence of cutting parameters on tool wear and surface roughness in hard turning of AISI H11 tool steel using ceramic tools, Int. J. Precis Eng. Manuf. 13 (2012) 1295–1302, https://doi.org/10.1007/s12541-012-0172-6.

[49] H. Aouici, M.A. Yallese, A. Belbah, M.F. Ameur, M. Elbah, Experimental investigation of cutting parameters influence on surface roughness and cutting forces in hard turning of X38CrMoV5-1 with CBN tool, Sadhana 38 (2013) 429–445, https://doi.org/10.1007/s12046-013-0147-z.

[50] M. Siva Surya, Optimization of turning parameters while turning Ti-6Al-4V titanium alloy for surface roughness and material removal rate using response surface methodology, Mater. Today Proc. 62 (2022) 3479–3484, https://doi.org/10.1016/j.matpr.2022.04.300.

[51] Parida A kumar, Das R, A.K. Sahoo, B.C Routara, Optimization of Cutting Parameters for Surface Roughness in Machining of gfrp Composites with Graphite/fly Ash Filler, Procedia Mater. Sci. 6 (2014) 1533–1538, https://doi.org/10.1016/j.mspro.2014.07.134.

[52] C. Jayaseelan, P. Padmanabhan, A. Athijayamani, K. Ramanathan, Effect of Machining Parameters on the Surface Roughness During Turning Operation in Banana Micro, Macro Particle and Short Fiber Reinforced Epoxy Composites, Period Di Mineral 91 (2022) 951–966, https://doi.org/10.37896/pd91.5/91569.

[53] M.Z. Hassan, E. Shakouri, P. Saraeian, Investigation of Surface Roughness in Turning of Epoxy-Glass Composite Tubes, Modares Mech. Eng. 16 (2017) 629–636.

[54] S. Abdur Rob, A.K Srivastava, Turning of Carbon Fiber Reinforced Polymer (CFRP) Composites: process Modeling and Optimization using Taguchi Analysis and Multi-Objective Genetic Algorithm, Manuf. Lett. 33 (2022) 29–40, https://doi.org/10.1016/j.mfglet.2022.07.012.

[55] V. Pragasam, H. Narayanaswamy, G. Balasubramania, P. Chinnaiyan, Investigation on Machining Characteristics of Banana Fiber and Silicon Carbide Reinforced Polymer Matrix Composites, Eng Trans. 68 (2020) 297–313.

[56] V. Bhardwaj, M. Gaur, V. Chaturvedi, S. Agrawal, Optimization of Machining Parameters for Nylon 6 Composite in CNC Lathe Using PCA-Based TOPSIS, Int J. Manuf. Mater. Process 4 (2018) 36–47.